


REVIEW ARTICLE **OPEN ACCESS**

Systematic Review of Radiomics and Artificial Intelligence in Intracranial Aneurysm Management

Monica-Rae Owens¹ | Samuel A. Tenhoeve¹ | Clayton Rawson² | Mohammed Azab³ | Michael Karsy⁴ ¹Spencer Fox Eccles School of Medicine, University of Utah, Salt Lake City, Utah, USA | ²College of Osteopathic Medicine, NOORDA College, Provo, Utah, USA | ³Kasr Al Ainy School of Medicine, Cairo University, Al Manial, Egypt | ⁴Department of Neurosurgery, University of Michigan, Ann Arbor, Michigan, USA**Correspondence:** Michael Karsy (mkarsy@med.umich.edu)**Received:** 26 December 2024 | **Revised:** 5 March 2025 | **Accepted:** 6 March 2025**Funding:** This research did not receive any specific grant from funding agencies in the public, commercial, or not-for-profit sectors.**Keywords:** aneurysm | artificial intelligence | deep learning | machine learning | radiomics | vascular

ABSTRACT

Intracranial aneurysms, with an annual incidence of 2%–3%, reflect a rare disease associated with significant mortality and morbidity risks when ruptured. Early detection, risk stratification of high-risk subgroups, and prediction of patient outcomes are important to treatment. Radiomics is an emerging field using the quantification of medical imaging to identify parameters beyond traditional radiology interpretation that may offer diagnostic or prognostic significance. The general radiomic workflow involves image normalization and segmentation, feature extraction, feature selection or dimensional reduction, training of a predictive model, and validation of the said model. Artificial intelligence (AI) techniques have shown increasing interest in applications toward vascular pathologies, with some commercially successful software including AiDoc, RapidAI, and Viz.AI, as well as the more recent Viz Aneurysm. We performed a systematic review of 684 articles and identified 84 articles exploring the applications of radiomics and AI in aneurysm treatment. Most studies were published between 2018 and 2024, with over half of articles in 2022 and 2023. Studies included categories such as aneurysm diagnosis (25.0%), rupture risk prediction (50.0%), growth rate prediction (4.8%), hemodynamic assessment (2.4%), clinical outcome prediction (11.9%), and occlusion or stenosis assessment (6.0%). Studies utilized molecular data (2.4%), radiologic data alone (51.2%), clinical data alone (28.6%), and combined radiologic and clinical data (17.9%). These results demonstrate the current status of this emerging and exciting field. An increased pace of innovation in this space is likely with the expansion of clinical applications of radiomics and AI in multiple vascular pathologies.

1 | Introduction

Intracranial aneurysms (IAs) pose a severe health threat, particularly during rupture, leading to subarachnoid hemorrhage. The annual incidence of unruptured aneurysms in the general populace is estimated between 2% and 3.2%, while IA ruptures account for nearly 5% of all strokes [1, 2]. The formation of IAs is influenced by multiple factors, including age, smoking,

and genetics [3]. Additionally, features such as irregular shape, aspect ratio, size, bottleneck factor, height-to-width ratio, and neck width may increase the likelihood of rupture [4, 5]. The rupture of IAs is a devastating event, carrying an estimated 12% prehospital mortality, 33% mortality within 48 h, and 50% mortality within 1 month [6]. Furthermore, at least half of those who survive are likely to experience severe disabilities, underscoring the critical need for effective rupture prediction [6].

This is an open access article under the terms of the [Creative Commons Attribution-NonCommercial](https://creativecommons.org/licenses/by-nc/4.0/) License, which permits use, distribution and reproduction in any medium, provided the original work is properly cited and is not used for commercial purposes.

© 2025 The Author(s). *Journal of Neuroimaging* published by Wiley Periodicals LLC on behalf of American Society of Neuroimaging.

Radiomics is a growing field that systematically quantifies basic and higher-order features from medical images, which can be used to predict clinical outcomes [7]. While the practice of radiomics is varied, it generally involves image normalization, segmentation, and processing, followed by feature extraction, selection, or dimensionality reduction [8]. Moreover, extracted features can be analyzed using various statistical and machine learning (ML) models to predict a wide variety of clinical outcomes. Artificial intelligence (AI), including supervised and unsupervised ML methods, as well as deep learning, has been applied toward the interpretation of increasingly complex sets of radiographic, clinical, and genomic data to better predict clinical outcomes.

The development and clinical implementation of AI in detecting aneurysm growth, progression, and eventual rupture may reduce patient mortality and long-term disability. We performed a systematic review evaluating the role of experimental AI algorithms, particularly radiomics, in the clinical management of IA. Particular attention was paid to predicting the rupture risk and aneurysm growth rate of IAs. By identifying key radiomics features and deep learning models that have shown high diagnostic and prognostic value, we hope to guide future clinical decision-making. Additionally, we aim to identify current gaps in the literature to facilitate future research in this area.

2 | Methods

2.1 | Data Collection

A literature search of PubMed was conducted using the following search terms: (deep learning) OR (machine learning) OR (radiomics) OR (convolutional neural network) OR (radiogenomics) OR (imaging genomics) AND (cerebral aneurysm or aneurysm). References from these articles were also reviewed to identify potentially relevant studies. This search returned 684 articles that were input into Rayyan AI software (Cambridge MA, <https://www.rayyan.ai/>) for the initial screening of titles and abstracts.

Initial screening was conducted by two independent reviewers (C.R. and M.A.). Any discrepancies were resolved by a third reviewer (M.O.). All three reviewers contributed to data extraction. Studies were excluded if they (1) were not specific to IAs, (2) evaluated detection without additional segmentation, feature extraction, other analysis, or outcome prediction, (3) did not assess rupture risk or growth rate, or (4) did not evaluate the use of radiomics. Additionally, review articles were excluded. The 84 included studies comprised English-only articles published between 2018 and June 2024 [9–93]. This systematic review was conducted in accordance with Preferred Reporting Items for Systematic reviews and Meta-Analyses guidelines. This review was registered with PROSPERO (CRD42024506886).

Full-text articles were reviewed to extract the author's year, sample size, pathology type, deep learning techniques, imaging modalities, and radiomics target (Tables 1–3). We categorized studies into two distinct groups: diagnosis and prediction. Diagnostic studies used radiomics to detect and diagnose IAs through advanced methods that could provide additional

diagnostic insights, while prediction studies used radiomics to predict either rupture risk or growth rate.

3 | Results

3.1 | Literature Search

A comprehensive literature search yielded 684 initial articles, of which 422 were excluded due to an irrelevant pathology focus, 77 did not meet the inclusion criteria, and 48 focused on detection methods without further analysis of rupture risk or growth rate. Additionally, 34 review articles and 17 studies that did not specifically apply radiomics or ML techniques were excluded. After these exclusions, 84 articles remained (Figure 1).

3.2 | Study Characteristics

Studies in this systematic review were published between 2018 and 2024, with a significant increase in publications after 2021, reflecting a recent surge in research interest. Notably, the years 2022 and 2023 alone accounted for over half of the reviewed studies, comprising 25.0% and 26.2%, respectively, of the total studies. This trend suggests a growing recognition of MLs' potential in enhancing the understanding and management of IAs.

We categorized the study outcomes into the following: diagnosis (25.0%), rupture risk prediction (50.0%), growth rate prediction (4.8%), hemodynamic assessment (2.4%), clinical outcome prediction (11.9%), and occlusion or stenosis assessment (6.0%) (Table 4). We also categorized the studies based on the data analyzed: molecular data (2.4%), radiologic data alone (51.2%), clinical data alone (28.6%), and combined radiologic and clinical data (17.9%). This breakdown reveals that while many studies relied solely on radiologic data, an increasing number have begun incorporating clinical data to provide a more comprehensive risk assessment.

3.3 | Imaging Modalities

Multiple imaging modalities evaluating aneurysms were studied. Digital subtraction angiography (DSA) was the most frequently used technique (31.0%), followed by CT angiography (CTA) (19.0%). Additional imaging modalities included 3-dimensional rotational angiography (3DRA; 9.5%), magnetic resonance angiography (4.8%), and high-resolution MRI (2.4%). A total of 20.2% of studies utilized a combination of these imaging techniques, while 13.1% of studies did not report specific imaging modalities used (Table 5).

4 | Discussion

4.1 | Overview of Pathologies, Techniques, Interventions, and Treatment Approaches

Aneurysm rupture was the most common outcome investigated, reflecting the critical need to identify patients at high risk and reduce morbidity. Additionally, several studies focused on aneurysm growth, which is another key factor in determining

TABLE 1 | Studies evaluating molecular and clinical–radiographic radiomic analyses in intracranial aneurysm treatment.

Author	Sample size	Techniques	Imaging used	Study findings
Molecular studies				
Maimaiti et al. [9]	21 UIA, 21 RIA, 16 normal	ML to assess DNA methylation	Unspecified	Correlation between DNA methylation and IA
Zhong et al. [10]	43 IA	Gene expression	Unspecified	Differentiating RIA vs. UIA
Clinical–radiological combined studies				
Jiang et al. [43]	112 IA	SVM, random forest, GLM	3DRA, DSA	Adding velocity informatics from aneurysmal velocity data can improve overall characterization of RIA
Xie et al. [40]	106 IA	CNN	CTA	Feature extraction
Liu et al. [46]	420 IA	ML predictive model	DSA	Flatness was the most important morphological determinant in predicting aneurysm stability
Yuan et al. [47]	Unspecified	Convolutional attention U-Net	MRA	Segmentation
Zhu et al. [48]	668 IA	Radiomics–morphological model for classification	CTA	Classifying RIA
Liang et al. [49]	281 IA	API-derived radiomics	DSA	Assessing treatment outcomes after embolization
Tong et al. [52]	254 IA	Morphology-based radiomics	DSA	Nomogram could predict rupture risk
Ou et al. [54]	122 IA	Radiomics	CTA	Predict rupture risk
Jadhav et al. [62]	81 IA	ML model	DSA	RF classifier found to be the most effective outcome predictor
Kong et al. [63]	118 IA	Radiomics nomogram model	TOF-MRA, DSA	Combined radiomics nomogram model outperformed both the clinical model and the radiomics model alone
Lv et al. [65]	65 IA	ML predictive model	DSA	ML models are effective in predicting wall enhancement in IA
Chen et al. [66]	807 patients	ML and regression	DSA, CTA	Hemodynamic factors improved rupture risk prediction; ML methods did not outperform LR
Ye et al. [80]	293 IA	Radiomics model	DSA, CTA	Combining radiomics with clinical factors can improve rupture risk prediction
Ma et al. [81]	64 IA	Radiomics	DSA	Potential use of radiomics in identifying after flow-diversion RIAs
Li et al. [89]	576 IA	Radiomics	CTA	Clinical–radscore model, combining radiomics features with clinical and inflammatory data predicting rupture
Veeturi et al. [93]	104 IA	Radiomics-based predictive nomogram	HR-MRI	Radscore-based nomogram, integrated radiomics and demographic data

Abbreviations: 3DRA, three-dimensional rotational angiography; API, angiographic parametric imaging; CNN, convolutional neural network; CTA, CT angiogram; DNA, deoxynucleic acid; DSA, digital subtraction angiogram; GLM, general linear model; HR, high-resolution; IA, intracranial aneurysm; LR, logistic regression; ML, machine learning; RF, random forest; RIA, ruptured intracranial aneurysm; SVM, support vector machine; TOF-MRA, time-of-flight MR angiogram; UIA, unruptured intracranial aneurysm.

TABLE 2 | Studies evaluating radiological radiomic analyses in intracranial aneurysm treatment.

Author	Sample size	Techniques	Imaging used	Study findings
Radiological studies				
An et al. [30]	125 IA	Multidimensional feature selection and construction	DSA	Combined models improved rupture risk assessment
Alwalid et al. [34]	393 IA	Radiomics model Rad score	CTA	Prediction of aneurysm rupture
Lin et al. [37]	322 IA	Multiple ML models	Unspecified	Multiple models predict rupture; aspect ratio was the leading predictor
Yang et al. [38]	576 IA	Radiomics, ML models	Unspecified	Predict RIA
Lin et al. [41]	425 IA	ML models	DSA	Predict recurrence after endovascular treatment, GBDT model showed best performance
Zhu et al. [56]	1897 IA	ML models	DSA	Undulation index, height–width ratio, and irregularity were most predictive of rupture
Lu et al. [57]	1029 IA	DL models	Unspecified	Prediction model performed better compared with classic clinical scale-based predictions
Paliwal et al. [60]	84 IA	ML models	DSA	Prediction of outcome after flow diversion; incorporated morphological, hemodynamic, and FD-device parameters; predicted 6-month occlusion outcome with 90% accuracy
Jin et al. [64]	354 IA	DNN models	2D DSA	Detecting and segmenting aneurysms
Feng et al. [67]	363 RIA, 535 UIA	3D CNN	CTA	13 key features predicted rupture
Li et al. [68]	227 patients, 254 IA	Radiomics	CTA	Integrated models are slightly better than a single model
Liu et al. [71]	403 MCA aneurysms	Nomogram	CTA	Nomogram generated for prediction of MCA rupture risk
Zeng et al. [72]	1237 IA training, 229 IA validation	CNN, DLM, and LR	CTA	LRM outperformed the DLM for predicting aneurysm stability
Cao et al. [73]	1246 IA	DL	3DRA	Structural relationship between the aneurysm and its parent vessel was key for predicting rupture
Irfan et al. [74]	400 IA	StrokeNet	2D DSA, 3DRA	Automated segmentation and rupture risk prediction, computed geometrical features, Fourier descriptors, and blood flow patterns
Shiraz et al. [75]	190 IA	DNN	DSA	API and DNN can predict IA occlusion
Veeturi et al. [76]	15 IA	SVM	DSA	Elevated WSS may contribute to wall thinning
Hadad et al. [77]	2265 IA	ML models	3DRA, CTA, MRA	Trained on cross-sectional data, identified aneurysms at risk of focal growth

(Continues)

TABLE 2 | (Continued)

Author	Sample size	Techniques	Imaging used	Study findings
Jin et al. [78]	52 IA	Radiomics	DSA	Elongation was identified as an independent predictor of ISS
Tong et al. [79]	660 IA	ML-based cluster analysis, LR models	DSA, CTA	Cluster and morphological factors predicted rupture
Guedon et al. [86]	146 IA	Predictive score	DSA	DIANES score is a predictive tool for occlusion after flow-diverter stent
Wisniewski et al. [88]	80 IA	API and DNN	DSA	Combination of multiple API parameters predicted treatment outcomes
Turhon et al. [92]	807 training, 200 internal validation, 108 external validation	ML model, LR model	CTA	Hemodynamic parameters improved prediction risk for UIAs
Liu et al. [97]	54 UIA, 540 RIA	Feed-forward ANN	CTA	Predicting risk of ACoA aneurysms
Ahn et al. [61]	457 UIA	ResNet50, CNN models	DSA	Diagnostic performance of multiview ResNet50 was better than other CNNs for predicting rupture risk

Abbreviations: 3DRA, three-dimensional rotational angiography; ACoA, anterior communicating artery; ANN, artificial neural network; API, angiographic parametric imaging; CNN, convolutional neural network; CTA, CT angiogram; DIANES score, IA diameter, indication, parent artery diameter ratio, neck ratio, side-branch artery, and sex; DL, deep learning; DLM, dynamic linear model; DNN, deep neural network; DSA, digital subtraction angiogram; FD, flow diversion; GBDT, gradient-boost decision tree; IA, intracranial aneurysm; ISS, in-stent stenosis; LR, logistic regression; LRM, large reconstruction model; MCA, middle cerebral artery; ML, machine learning; MRA, magnetic resonance angiogram; RIA, ruptured intracranial aneurysm; SVM, support vector machine; UIA, unruptured intracranial aneurysm; WSS, wall shear stress.

TABLE 3 | Studies evaluating primarily clinical outcomes in radiomic studies on intracranial aneurysm treatment.

Author	Sample size	Techniques	Imaging used	Study findings
Clinical studies				
Mu et al. [53]	112 IA	ML models	3DRA	Prediction of IA rupture risk
Ludwig et al. [55]	353 IA	Radiomics	3DRA	Radiomics elongation and flatness features were the best performers of rupture status
Wu et al. [58]	1508 IA	Cascade detection and classification models	CTA	Developed feasible pipeline for clinical use to assist radiologists in aneurysm detection and classification of RIA vs. UIA
Li et al. [59]	1325 IA	ML model	Unspecified	Hemorrhagic stroke history and gender predicted single ACoA rupture
Tian et al. [69]	443 IA	ML models	DSA	Distal aneurysm location, size, and treatment modality predicted treatment complications
Zador et al. [82]	226 IA	Multivariate and Bayesian network	CTA, DSA	Combining LR and Bayesian networks showed that WFNS grade and age were the most influential predictors of outcome

Abbreviations: 3DRA, three-dimensional rotational angiography; ACoA, anterior communicating artery; CTA, CT angiogram; DSA, digital subtraction angiogram; IA, intracranial aneurysm; LR, logistic regression; ML, machine learning; RIA, ruptured intracranial aneurysm; UIA, unruptured intracranial aneurysm; WFNS, World Federation of Neurosurgical Societies.

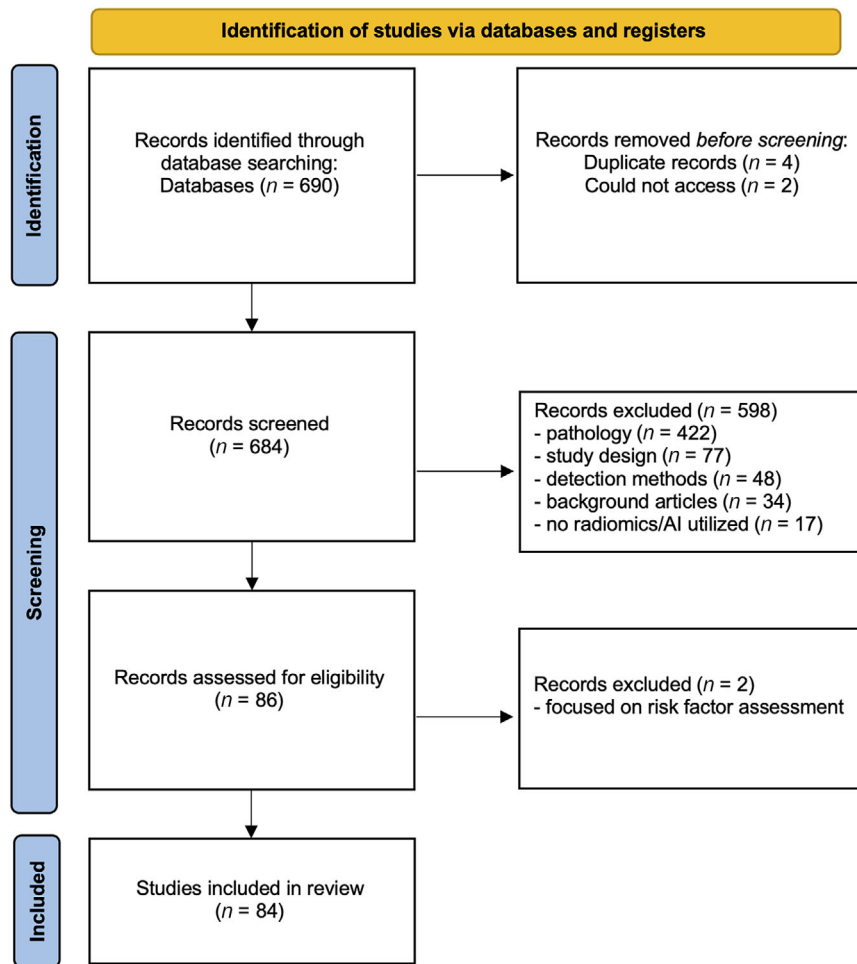


FIGURE 1 | Flowchart of studies screened, included, and excluded (Preferred Reporting Items for Systematic reviews and Meta-Analyses diagram). AI, artificial intelligence; *n*, number of papers.

TABLE 4 | Primary objectives in radiomics and other artificial intelligence techniques.

Objective	Number of studies (%)
Rupture risk prediction	42 (50.0%)
Diagnosis	21 (25.0%)
Clinical outcome prediction	10 (11.9%)
Occlusion or stenosis assessment	5 (6.0%)
Growth rate prediction	4 (4.8%)
Hemodynamic assessment	2 (2.4%)

rupture risk over time. Techniques employed to assess these pathologies varied but generally included quantitative imaging approaches to extract data from structural and morphological features in aneurysm imaging.

The studies also secondarily explored a range of treatment interventions and treatment-related assessments. Some studies evaluated the impact of endovascular treatments, such as coil embolization and flow-diverting stents, on radiomic features, allowing researchers to explore how treatment-induced changes

TABLE 5 | Distribution of imaging modalities utilized.

Imaging modality	# of studies utilizing modality (%)
DSA	26 (31.0%)
Combination	17 (20.2%)
CTA	16 (19.0%)
Unspecified	11 (13.1)
3DRA	8 (9.5%)
MRA	4 (4.8%)
HR-MRI	2 (2.4%)

Abbreviations: 3DRA, three-dimensional rotational angiography; CTA, CT angiogram; DSA, digital subtraction angiogram; HR-MRI, high-resolution magnetic resonance imaging; MRA, magnetic resonance angiogram.

in aneurysm morphology and structure may affect future risk assessments. This examination of treatment-related imaging provides valuable insights into postintervention monitoring and the potential for radiomics to assess treatment efficacy. Other studies examined clinical outcomes, including patient prognosis following treatment or observed over a specified follow-up period.

4.2 | Analytical AI Models

Various analytic models evaluated in aneurysms included convolutional neural networks (CNNs), support vector machines (SVMs), logistic regression (LR), and random forests (RFs). Advanced ML models, such as Light Gradient Boosting Machine (LGBM) and eXtreme Gradient Boosting (XGBoost), were employed in several studies.

4.3 | Genomics Analysis of Aneurysm Outcomes

Several studies aimed to incorporate molecular features of aneurysms into clinical decision-making. Maimaiti et al. utilized multiomics and epigenome-wide association studies to analyze correlations between deoxyribonucleic acid (DNA) methylation and IA predisposition [9]. The study included 21 unruptured IAs, 21 ruptured IAs, and 16 normal intracranial artery samples. Analysis of different DNA methylation-related genes (MRGs) identified 19 genes, including *Mdb3* and *Zbtb38*, which exhibited high endothelial cell and fibroblast expression. A total of 100 ML models were developed utilizing a training set cohort and two external validation cohorts to analyze these MRGs and their capability of constructing a predictive model for aneurysm rupture. Analysis used integrated ML, expression quantitative trait loci, methylation quantitative trait loci, Mendelian regression, and summary-data-based Mendelian randomization. The receiver operating characteristic curve and decision curve analysis were used to assess model performance, showing good discrimination between cohorts. Of the 100 models developed, 14 models achieved perfect performance accuracy (1.00), demonstrating a high correlation of these genomic models with both unruptured and ruptured IAs.

Another study evaluated differential gene expression in IA treatment using a sample population of 43 IAs subdivided into two datasets to identify specific Hub genes (spermine synthase, macrophage receptor with collagenous structure, zymogen granule protein 16B, and LIM and calponin homology domains 1) [10]. Subgroup I consisted of a higher rupture risk, while subgroup II contained 70% unruptured aneurysms. A predictive model was developed based on these Hub genes, using LGBM (area under the curve [AUC]: 0.92; precision-recall [PR]: 0.888), XGBoost (AUC: 0.983; PR: 0.984), and LR algorithms (AUC: 0.942; PR: 0.92). This predictive model was validated using data from one of the selected datasets and was found to have good diagnostic performance in differentiating unruptured and ruptured IAs. Additionally, monocytic lineage was found to be a significant factor in intracranial rupture ($p < 0.05$), with an abundance of monocytes and neutrophils found in ruptured IAs compared to unruptured. Additionally, all Hub genes were found to be significantly associated with monocytic lineage. These findings are consistent with previous literature highlighting the increased expression of monocyte chemoattractant protein-1 in IA rupture [94, 95].

4.4 | Prediction of Rupture Risk

A study utilizing CNN sought to predict the rupture risk of IAs, focusing on hemodynamic parameters such as wall shear stress (WSS), wall strain (WS), and a combination of WSS and WS [12]. These parameters were initially calculated using fluid-structure

interactions and computational fluid dynamics, which were then employed to train and test a CNN. The model trained using WSS had an AUC value of 0.716 (sensitivity: 0.5, specificity: 0.79); the model trained using WS had an AUC value of 0.741 (sensitivity: 0.74, specificity: 0.71); and the model utilizing combined WSS/WS images had an AUC value of 0.883 (sensitivity: 0.81, specificity: 0.82), representing a more effective tool for predicting rupture risk in IAs.

Li and colleagues devised a multiscale 3D CNN using CTA, termed TransIAR net, to better predict rupture risk than manual measurements [15]. This model was able to extract the structural patterns of the aneurysm and its surrounding structures, resulting in a 10%–15% improvement in the accuracy of rupture status prediction. Accuracy measurements were measured through a comparison of clinical diagnosis between neuroradiologists, TransIAR, and TransIAR with added auxiliary features (TransIAR^{AF}). The accuracy for the two trained neuroradiologists was 82.90 and 87.80, while TransIAR and TransIAR^{AF} showed accuracies of 89.02 and 91.46, respectively. The AUC for the neuroradiologists was 73.20 and 76.80, while for TransIAR and TransIAR^{AF}, it was 92.15 and 92.09, respectively. Additionally, the diagnosis times for the two neuroradiologists were 57 and 62 min, while for TransIAR and TransIAR^{AF}, the algorithm could be completed in 3.46 and 3.47 s, respectively. This ML method was found to be significantly more accurate and efficient than human-based predictions within the test datasets of this study. Nevertheless, important limitations to consider include the significant amount of time spent by neuroradiologists in performing precise measurements. Additionally, due to reliance on human input, there is a significant amount of variation and uncertainty within the data.

Hu et al. focused on the detection of aneurysms and the analysis of rupture risk using DSA [39]. A total of 263 aneurysms were analyzed using a Bayesian optimization filter for aneurysm detection, focusing on variations in blood flow and morphology. Additionally, they were able to extract intensity, texture, and hemodynamic features from the detected aneurysms to differentiate between ruptured ($n = 125$) and unruptured ($n = 138$) aneurysms. The classification of this model yielded accuracy, sensitivity, specificity, and AUC values of 96.1%, 94.4%, 97.5%, and 0.982, respectively, indicating a reliable method for aneurysm detection and rupture prediction.

A study conducted by Niemann et al. proposed a semantic graph segmentation and centerline extraction to improve the analysis of aneurysm rupture risk [13]. A deep learning-based model was developed for mesh segmentation, generating a detailed abstract graphical representation, aiming to improve aneurysm classification, rupture prediction, and hemodynamic evaluation. They found that vessels in close proximity to ruptured aneurysms exhibited higher average torsion and curvature compared to vessels near unruptured aneurysms. The test accuracy of the mesh segmentation reached 83.3% for the classification of the rupture state; however, there were different segmentation components that were analyzed. Segmentation accuracy for vessels, aneurysms, inlets, and bifurcations was 74.8%, 71.4%, 69.8%, and 37.0%, respectively. This model proved to be useful for morphologic and hemodynamic parameter extraction; however, the database used for mesh classification is relatively small

and must therefore be validated using a more robust study sample.

4.5 | Evaluating the Impact of Therapies

Another study looked at the use of deep learning to predict hemodynamics before and after flow-diversion stent placement in IAs [36]. A deep learning network employed a flexible point cloud format representing the geometry and flow distribution of aneurysms before and after stent placement. This method avoided the need for complex computational fluid dynamics calculations. The authors showed comparability to computational fluid dynamics with significantly reduced computational time by a factor of 1800. The limitations of this study include a lack of data on real patients, as well as limited application due to only analyzing sidewall aneurysms.

An integrated model using computational fluid dynamics and a combination of deep learning and ML algorithms was developed to classify ruptured ($n = 39$) and unruptured ($n = 109$) aneurysms [25]. The ML models comprised RF, k -nearest neighbor (KNN), XGBoost, SVM, and LGBM. To extract hemodynamic cloud features, a Pointnet deep learning algorithm was applied. The classification accuracy of RF, KNN, XGBoost, SVM, and LightGBM was 0.824, 0.759, 0.839, 0.860, and 0.829, respectively. With consideration of hemodynamic cloud features, the SVM model outperformed the other models, with accuracy and AUC values of 0.926 and 0.969, respectively.

In addition to rupture risk prediction, one study looked into treatment outcome prediction using an automated ML-based model (AutoML) [22]. Patients who were endovascularly treated were considered to have successful treatment if complete occlusion of the aneurysm was observed at follow-up. Three models were developed including a statistical prediction model using multivariate LR, a manual model, and an AutoML model. These models were compared based on their area under the precision-recall curve (AUPRC) and area under the receiver operating characteristic curve (AUROC) values. The AUPRC and AUROC values for the statistical model were 0.432 and 0.745, respectively. The manual model showed AUPRC and AUROC values of 0.545 and 0.781, respectively. The AutoML model outperformed the other two models, with AUPRC and AUROC values of 0.632 and 0.832, respectively. These findings support the feasibility of using AutoML to predict treatment outcomes for patients with IAs, which is consistent with current literature on ML-based models.

The use of 3DRA was employed by Lauric et al., who sought to identify an efficient, operator-independent methodology for rupture status classification compared to conventional radiomics. A total of 135 sidewall (32 ruptured) and 216 bifurcation (90 ruptured) aneurysms were analyzed from 3DRA images [29]. Findings suggest that enhanced radiomics utilizing neck orientation and parent vessel estimation is an efficient operator-independent method for classifying both sidewall and bifurcation aneurysm rupture risk. These findings are consistent with another study done by Cao et al., who developed a point cloud-based deep learning model that could effectively capture the morphological aspects and spatial contour of aneurysms, enhanced by parent vessel utilization [73].

4.6 | Predicting Clinical Outcomes

Another interesting study done by Peng et al. used ML predictive models to assess postoperative neurological function by using preoperative CTA imaging data to predict postembolization Hunt–Hess scores [45]. Three distinct approaches were used, including a radiomics model, a deep learning model, and a combined deep learning–radiomics model. The AUC and Matthews correlation coefficient (MCC) values for the radiomic model were 0.935 and 0.793, respectively. The AUC and MCC values for the deep learning model were 0.959 and 0.815, respectively. The AUC and MCC values for the combined model were 0.968 and 0.820, respectively. These values indicate that the fusion-based model exhibited the highest predictive performance compared to the other two models. However, this was a single-center study with a relatively small sample size, limiting the robustness and applicability of the findings of this study.

4.7 | Aneurysm Detection

Another study focused on image segmentation using a self-supervised, pretrained deep learning model to learn deep embeddings of aneurysm morphology from 947 unlabeled radiographic images [16]. This model was trained with 120 labeled cases of known rupture status integrated with clinical information to further improve rupture prediction. An assistive diagnosis system was also developed and tested with five neurosurgeons. This model reached an AUC value of 0.823 prior to clinical data integration, which was then improved to $AUC = 0.853$. Additionally, this assistive diagnosis system significantly improved the performance accuracy of neurosurgeons, with an improved AUC from 0.877 to 0.945 ($p = 0.037$), indicating strong diagnostic utility. This finding emphasizes the potential impact of assistive technologies in aiding clinicians in clinical evaluation and decision-making to enhance patient outcomes.

Podgorsak et al. utilized angiographic parametric imaging and DSA in combination with CNN to automatically identify and segment saccular aneurysms from surrounding vasculature [20]. They retrospectively collected 350 angiographic images of IAs that were input to a CNN tasked with semantic segmentation. This model was assessed for accuracy using the Dice similarity coefficient (DSC) and Jaccard index (JI) for both the aneurysms and their surrounding vasculature. The mean JI for the aneurysms and vasculature was 0.823 (95% confidence interval [CI]: 0.783–0.863) and 0.737 (95% CI: 0.682–0.792), respectively. The mean DSC was 0.903 (95% CI: 0.867–0.937) and 0.849 (95% CI: 0.811–0.887), respectively. The mean AUROC was 0.791 (95% CI: 0.740–0.817) and 0.715 (95% CI: 0.678–0.733), respectively. The findings of this study were comparable to manually contoured masks, suggesting that this method is noninferior to previous studies' findings.

4.8 | Combined Clinical and Radiologic Data

Combined clinical and radiomics data are an effective approach to the management and treatment of IAs, enhancing diagnostic accuracy, improving risk stratification, and providing a comprehensive view of patients' conditions. One study by Ye

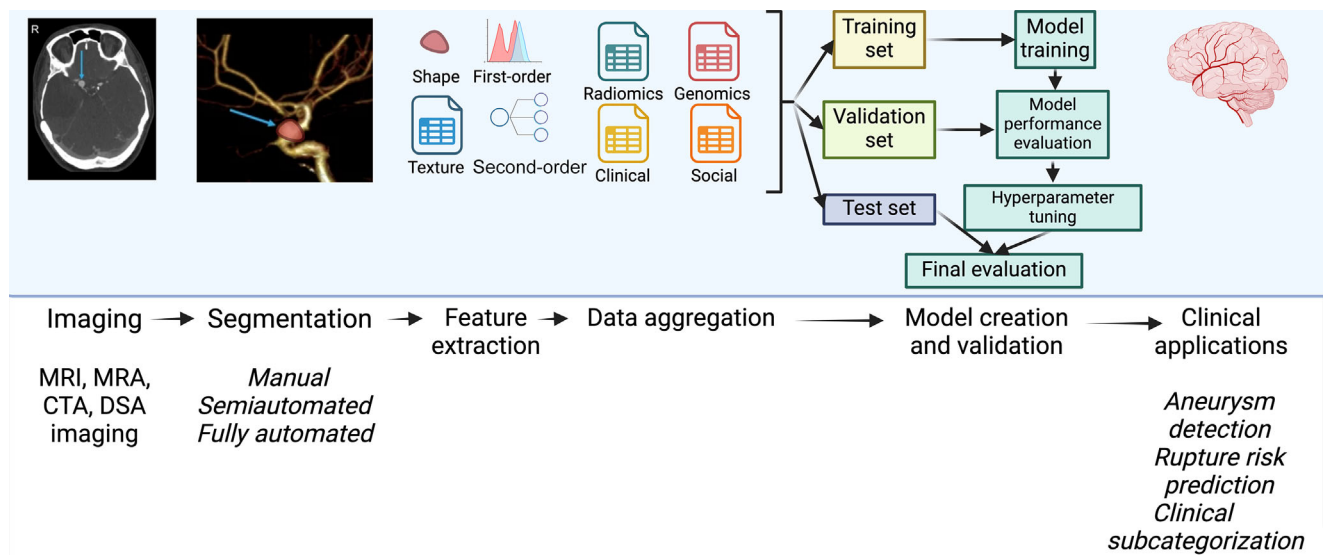


FIGURE 2 | Overview of strategies for radiomics and machine learning in aneurysm treatment. Various steps of using radiomics or machine learning in the clinical management of aneurysm treatment are shown. Inputting and normalization of clinical and radiographic data are first essential. Radiographic data must be representative of the eventual testing group the model will be applied toward. Radiographic data require automated, semiautomated, or manual segmentation for model training. Feature extraction and generation of a predictive model are performed with both internal testing of a model’s consistency (e.g., hyperparameter tuning, model performance evaluation) and external testing. Lastly, integration of a model into clinical workflow is crucial to encourage adoption by clinicians. CTA, computed tomography angiography; DSA, digital subtraction angiography; MRA, magnetic resonance angiography.

et al. looked at predictive models to accurately identify small aneurysms (<5 mm) with a low risk of rupture, based on clinical risk factors and radiomics signatures [80]. They developed a combined clinical–radiomics model (AUC = 0.85) constructed by nomogram analysis, which was found to outperform both the conventional radiomics model (AUC = 0.75) and the clinical model (AUC = 0.74), demonstrating the effectiveness of combining both clinical and radiomics data for predicting rupture status and facilitating effective clinical decision-making. This study, however, was a single-center study with a relatively small study population. Additionally, these findings were not validated using an external validation cohort, limiting the robustness and generalizability of these findings.

Another study focused on the classification of rupture risk for small IAs (<5 mm) and derived and validated an ML-based prediction model by combining clinical, morphological, and hemodynamic information [21]. This model looked at 504 consecutive patients, with only small aneurysms detected on CTA and invasive cerebral angiography, which were split into a training group (81%) and an internal validation group (19%). ML models included SVM, RF, LR, and multilayer perceptron. The SVM outperformed the other model, with AUC values of 0.88 and 0.91 in the training and internal validation datasets, respectively, indicating the generalizability of these findings. Additionally, the best predictors of aneurysm rupture included hemodynamic parameters, stable flow patterns, concentrated inflow streams, a small (<50%) flow-impingement zone, and oscillatory shear index coefficient of variation.

A pilot study using an ML-based approach for predicting aneurysm wall enhancement evaluated hemodynamic and morphological parameters along with clinical risk factors [65]. The

PHASES score, a risk assessment tool for predicting aneurysm rupture, estimates risk through a multifactorial approach combining clinical and anatomical features [96]. Lv et al. [65] employed nine ML models that were applied to 65 aneurysm cases with various predictor variables. The model based on gradient boosting had an AUC value of 0.98, performing the best compared to the other models. The generalized linear model (AUC = 0.80) was the second-best-performing model. The dominant predictor for wall enhancement was size ratio, closely followed by the PHASES score and mean WSS.

Another model that combined clinical and radiomics models to predict the outcome of aneurysm treatment developed an ML model to predict residual flow based on over 100 clinical and imaging features, focused on predicting outcomes of wide-neck bifurcation aneurysms treated with an intrasaccular embolization device, Woven EndoBridge (WEB) [62]. This neural network segmentation algorithm was found to have a 90% overlap with conventional manual contouring in 2D and an 83% overlap in 3D, proving accurate in classifying complete versus partial occlusion outcomes after WEB implantation with an accuracy of 75.31%.

4.9 | Limitations and Future Direction

The findings of our study indicate a promising outlook for the future use of radiomics in aneurysm research. At present, there are only a few commercially available radiomics and ML imaging tools in clinical settings (e.g., Viz Aneurysm, AiDoc, RapidAI). Two of the most popular software, Viz Aneurysm and RapidAI, aim to improve the detection and measurement of unruptured aneurysms in conjunction with radiology interpretation. Our investigation indicated a variety of experimental methods for

radiomic feature extraction and ML application, often with internal validation via single-center datasets. We identified a general trend toward enhanced computational analysis and applications over time. Weaknesses of these algorithms include the potential for false positives and the need to improve accuracy given the high risk of intracerebral aneurysms. Potential solutions include standardizing research methodologies across studies, utilizing multicenter data to address image variability and disease heterogeneity, and validating models using independent external data. For algorithms to be genuinely dependable in clinical situations, prospective studies are essential.

5 | Conclusions

Radiomics plays a key role in the diagnosis, management, treatment, and outcome prediction of IAs (Figure 2). By analyzing morphologic and hemodynamic features and integrating these data with clinical risk factors, radiomics enhances the ability to identify aneurysms, analyze their structural characteristics, and predict their behavior. This comprehensive strategy allows clinicians to improve risk stratification and implement tailored treatment strategies through a multimodal approach, thereby enhancing outcomes and guiding clinical decision-making. Additionally, incorporating radiomic features with clinical data shows significant promise, as supported by current research. The integration of radiomics into routine IA treatment will refine decision-making processes and optimize surgical interventions for patients with this complex pathology.

Acknowledgments

The author has nothing to report.

Conflicts of Interest

Michael Karsy reports consulting with Altus. The other authors declare no conflicts of interest.

References

1. A. S. Deshmukh, S. M. Priola, A. H. Katsanos, et al., "The Management of Intracranial Aneurysms: Current Trends and Future Directions," *Neurology International* 16, no. 1 (2024): 74–94.
2. J. van Gijn, R. S. Kerr, and G. J. Rinkel, "Subarachnoid Haemorrhage," *Lancet* 369, no. 9558 (2007): 306–318.
3. W. Brinjikji, Y. Q. Zhu, G. Lanzino, et al., "Risk Factors for Growth of Intracranial Aneurysms: A Systematic Review and Meta-Analysis," *American Journal of Neuroradiology* 37, no. 4 (2016): 615–620.
4. R. Kleinloog, N. de Mul, B. H. Verweij, J. A. Post, G. J. E. Rinkel, and Y. M. Ruigrok, "Risk Factors for Intracranial Aneurysm Rupture: A Systematic Review," *Neurosurgery* 82, no. 4 (2018): 431–440.
5. G. X. Wang, D. Zhang, Z. P. Wang, L. Q. Yang, H. Yang, and W. Li, "Risk Factors for Ruptured Intracranial Aneurysms," *Indian Journal of Medical Research* 147, no. 1 (2018): 51–57.
6. F. A. Sehba, J. Hou, R. M. Pluta, and J. H. Zhang, "The Importance of Early Brain Injury After Subarachnoid Hemorrhage," *Progress in Neurobiology* 97, no. 1 (2012): 14–37.
7. C. Scapicchio, M. Gabelloni, A. Barucci, D. Cioni, L. Saba, and E. Neri, "A Deep Look into Radiomics," *Radiology Medical* 126, no. 10 (2021): 1296–1311.

8. J. E. van Timmeren, D. Cester, S. Tanadini-Lang, H. Alkadhi, and B. Baessler, "Radiomics in Medical Imaging—"How-to" Guide and Critical Reflection," *Insights Imaging* 11, no. 1 (2020): 91.
9. A. Maimaiti, M. Turhon, A. Abulaiti, et al., "DNA Methylation Regulator-Mediated Modification Patterns and Risk of Intracranial Aneurysm: A Multi-Omics and Epigenome-Wide Association Study Integrating Machine Learning, Mendelian Randomization, eQTL and mQTL Data," *Journal of Translational Medicine* 21, no. 1 (2023): 660.
10. A. Zhong, F. Wang, Y. Zhou, N. Ding, G. Yang, and X. Chai, "Molecular Subtypes and Machine Learning-Based Predictive Models for Intracranial Aneurysm Rupture," *World Neurosurgery* 179 (2023): e166–e186.
11. X. Lei and Y. Yang, "Deep Learning-Based Magnetic Resonance Imaging in Diagnosis and Treatment of Intracranial Aneurysm," *Computational and Mathematical Methods in Medicine* 2022 (2022): 1683475.
12. H. Yang, C. Kwang-Chun, K. Jung-Jae, K. Jae Ho, K. Yong Bae, and J. H. Oh, "Rupture Risk Prediction of Cerebral Aneurysms Using a Novel Convolutional Neural Network-Based Deep Learning Model," *Journal of NeuroInterventional Surgery* 15, no. 2 (2023): 200–204.
13. A. Niemann, D. Behme, N. Larsen, B. Preim, and S. Saalfeld, "Deep Learning-Based Semantic Vessel Graph Extraction for Intracranial Aneurysm Rupture Risk Management," *International Journal of Computer Assisted Radiology and Surgery* 18, no. 3 (2023): 517–525.
14. H. Nishi, N. M. Cancelliere, A. Rustici, et al., "Deep Learning-Based Cerebral Aneurysm Segmentation and Morphological Analysis With Three-Dimensional Rotational Angiography," *Journal of NeuroInterventional Surgery* 16, no. 2 (2024): 197–203.
15. P. Li, Y. Liu, J. Zhou, et al., "A Deep-Learning Method for the End-to-End Prediction of Intracranial Aneurysm Rupture Risk," *Patterns* 4, no. 4 (2023): 100709.
16. C. Ou, C. Li, Y. Qian, et al., "Morphology-Aware Multi-Source Fusion-Based Intracranial Aneurysms Rupture Prediction," *European Radiology* 32, no. 8 (2022): 5633–5641.
17. M. Chen, C. Geng, D. Wang, et al., "A Coarse-to-Fine Cascade Deep Learning Neural Network for Segmenting Cerebral Aneurysms in Time-of-Flight Magnetic Resonance Angiography," *Biomedical Engineering Online* 21, no. 1 (2022): 71.
18. S. Tanioka, F. Ishida, A. Yamamoto, et al., "Machine Learning Classification of Cerebral Aneurysm Rupture Status With Morphologic Variables and Hemodynamic Parameters," *Radiology Artificial Intelligence* 2, no. 1 (2020): e190077.
19. F. J. Detmer, D. Lückehe, F. Mut, et al., "Comparison of Statistical Learning Approaches for Cerebral Aneurysm Rupture Assessment," *International Journal of Computer Assisted Radiology and Surgery* 15, no. 1 (2020): 141–150.
20. A. R. Podgorsak, R. A. Rava, M. M. Shiraz Bhurwani, et al., "Automatic Radiomic Feature Extraction Using Deep Learning for Angiographic Parametric Imaging of Intracranial Aneurysms," *Journal of NeuroInterventional Surgery* 12, no. 4 (2020): 417–421.
21. Z. Shi, G. Z. Chen, L. Mao, et al., "Machine Learning-Based Prediction of Small Intracranial Aneurysm Rupture Status Using CTA-Derived Hemodynamics: A Multicenter Study," *Ajnr American Journal of Neuroradiology* 42, no. 4 (2021): 648–654.
22. C. Ou, J. Liu, Y. Qian, et al., "Automated Machine Learning Model Development for Intracranial Aneurysm Treatment Outcome Prediction: A Feasibility Study," *Frontiers in Neurology* 12 (2021): 735142.
23. B. Joo, H. S. Choi, S. S. Ahn, et al., "A Deep Learning Model With High Standalone Performance for Diagnosis of Unruptured Intracranial Aneurysm," *Yonsei Medical Journal* 62, no. 11 (2021): 1052–1061.
24. W. Xiong, T. Chen, J. Li, et al., "Interpretable Machine Learning Model to Predict Rupture of Small Intracranial Aneurysms and Facilitate Clinical Decision," *Neurological Sciences* 43, no. 11 (2022): 6371–6379.
25. R. Chen, X. Mo, Z. Chen, P. Feng, and H. Li, "An Integrated Model Combining Machine Learning and Deep Learning Algorithms for

- Classification of Rupture Status of IAs,” *Frontiers in Neurology* 13 (2022): 868395.
26. S. F. Salimi Ashkezari, F. Mut, M. Slawski, C. M. Jimenez, A. M. Robertson, and J. R. Cebal, “Identification of Small, Regularly Shaped Cerebral Aneurysms Prone to Rupture,” *AJNR American Journal of Neuroradiology* 43, no. 4 (2022): 547–553.
 27. D. Wei, D. Deng, S. Gui, et al., “Machine Learning to Predict In-Stent Stenosis After Pipeline Embolization Device Placement,” *Frontiers in Neurology* 13 (2022): 912984.
 28. M. A. Silva, J. Patel, V. Kavouridis, et al., “Machine Learning Models Can Detect Aneurysm Rupture and Identify Clinical Features Associated With Rupture,” *World Neurosurgery* 131 (2019): e46–e51.
 29. A. Lauric, C. G. Ludwig, and A. M. Malek, “Enhanced Radiomics for Prediction of Rupture Status in Cerebral Aneurysms,” *World Neurosurgery* 159 (2022): e8–e22.
 30. X. An, J. He, Y. Di, et al., “Intracranial Aneurysm Rupture Risk Estimation With Multidimensional Feature Fusion,” *Frontiers in Neuroscience* 16 (2022): 813056.
 31. C. Ou, J. Liu, Y. Qian, et al., “Rupture Risk Assessment for Cerebral Aneurysm Using Interpretable Machine Learning on Multidimensional Data,” *Frontiers in Neurology* 11 (2020): 570181.
 32. H. C. Kim, J. K. Rhim, J. H. Ahn, et al., “Machine Learning Application for Rupture Risk Assessment in Small-Sized Intracranial Aneurysm,” *Journal of Clinical Medicine* 8, no. 5 (2019): 683.
 33. Ž Bizjak, F. Pernuš, and Ž Špiclin, “Deep Shape Features for Predicting Future Intracranial Aneurysm Growth,” *Frontiers in Physiology* 12 (2021): 644349.
 34. O. Alwalid, X. Long, M. Xie, et al., “CT Angiography-Based Radiomics for Classification of Intracranial Aneurysm Rupture,” *Frontiers in Neurology* 12 (2021): 619864.
 35. J. N. Stember, P. Chang, D. M. Stember, et al., “Convolutional Neural Networks for the Detection and Measurement of Cerebral Aneurysms on Magnetic Resonance Angiography,” *Journal of Digital Imaging* 32, no. 5 (2019): 808–815.
 36. G. Li, X. Song, H. Wang, et al., “Prediction of Cerebral Aneurysm Hemodynamics With Porous-Medium Models of Flow-Diverting Stents via Deep Learning,” *Frontiers in Physiology* 12 (2021): 733444.
 37. M. Lin, N. Xia, R. Lin, et al., “Machine Learning Prediction Model for the Rupture Status of Middle Cerebral Artery Aneurysm in Patients With Hypertension: A Chinese Multicenter Study,” *Quantitative Imaging in Medicine and Surgery* 13, no. 8 (2023): 4867–4878.
 38. B. Yang, W. Li, X. Wu, et al., “Comparison of Ruptured Intracranial Aneurysms Identification Using Different Machine Learning Algorithms and Radiomics,” *Diagnostics* 13, no. 16 (2023): 2627.
 39. T. Hu, H. Yang, and W. Ni, “A Framework for Intracranial Aneurysm Detection and Rupture Analysis on DSA,” *Journal of Clinical Neuroscience* 115 (2023): 101–107.
 40. Y. Xie, S. Liu, H. Lin, et al., “Automatic Risk Prediction of Intracranial Aneurysm on CTA Image With Convolutional Neural Networks and Radiomics Analysis,” *Frontiers in Neurology* 14 (2023): 1126949.
 41. S. Lin, Y. Zou, J. Hu, et al., “Development and Assessment of Machine Learning Models for Predicting Recurrence Risk After Endovascular Treatment in Patients With Intracranial Aneurysms,” *Neurosurgical Review* 45, no. 2 (2022): 1521–1531.
 42. M. Rezaeitalshmahalleh, Z. Lyu, N. Mu, and J. Jiang, “Using Convolutional Neural Network-Based Segmentation for Image-Based Computational Fluid Dynamics Simulations of Brain Aneurysms: Initial Experience in Automated Model Creation,” *Journal of Mechanics in Medicine and Biology* 23, no. 4 (2023): 2340055.
 43. J. Jiang, M. Rezaeitalshmahalleh, Z. Lyu, et al., “Augmenting Prediction of Intracranial Aneurysms’ Risk Status Using Velocity-Informatics: Initial Experience,” *Journal of Cardiovascular Translational Research* 16, no. 5 (2023): 1153–1165.
 44. N. Stroh, H. Stefanits, A. Maletzky, et al., “Machine Learning Based Outcome Prediction of Microsurgically Treated Unruptured Intracranial Aneurysms,” *Scientific Reports* 13, no. 1 (2023): 22641.
 45. Y. Peng, Y. Wang, Z. Wen, et al., “Deep Learning and Machine Learning Predictive Models for Neurological Function After Interventional Embolization of Intracranial Aneurysms,” *Frontiers in Neurology* 15 (2024): 1321923.
 46. Q. Liu, P. Jiang, Y. Jiang, et al., “Prediction of Aneurysm Stability Using a Machine Learning Model Based on PyRadiomics-Derived Morphological Features,” *Stroke; A Journal of Cerebral Circulation* 50, no. 9 (2019): 2314–2321.
 47. W. Yuan, Y. Peng, Y. Guo, Y. Ren, and Q. Xue, “DCAU-Net: Dense Convolutional Attention U-Net for Segmentation of Intracranial Aneurysm Images,” *Visual Computing for Industry, Biomedicine, and Art* 5, no. 1 (2022): 9.
 48. D. Zhu, Y. Chen, K. Zheng, et al., “Classifying Ruptured Middle Cerebral Artery Aneurysms With a Machine Learning Based, Radiomics-Morphological Model: A Multicenter Study,” *Frontiers in Neuroscience* 15 (2021): 721268.
 49. F. Liang, C. Ma, H. Zhu, et al., “Using Angiographic Parametric Imaging-Derived Radiomics Features to Predict Complications and Embolization Outcomes of Intracranial Aneurysms Treated by Pipeline Embolization Devices,” *Journal of NeuroInterventional Surgery* 14, no. 8 (2022): 826–831.
 50. N. Amigo, A. Valencia, W. Wu, S. Patnaik, and E. Finol, “Cerebral Aneurysm Rupture Status Classification Using Statistical and Machine Learning Methods,” *Proceedings of the Institution of Mechanical Engineers Part H* 235, no. 6 (2021): 655–662.
 51. T. Lu, Y. He, Z. Liu, et al., “A Machine Learning-Derived Gene Signature for Assessing Rupture Risk and Circulatory Immunopathologic Landscape in Patients With Intracranial Aneurysms,” *Frontiers in Cardiovascular Medicine* 10 (2023): 1075584.
 52. X. Tong, X. Feng, F. Peng, et al., “Morphology-Based Radiomics Signature: A Novel Determinant to Identify Multiple Intracranial Aneurysms Rupture,” *Aging* 13, no. 9 (2021): 13195–13210.
 53. N. Mu, M. Rezaeitalshmahalleh, Z. Lyu, et al., “Can We Explain Machine Learning-Based Prediction for Rupture Status Assessments of Intracranial Aneurysms?,” *Biomedical Physics & Engineering Express* 9, no. 3 (2023): 037001.
 54. C. Ou, W. Chong, C. Z. Duan, X. Zhang, M. Morgan, and Y. Qian, “A Preliminary Investigation of Radiomics Differences Between Ruptured and Unruptured Intracranial Aneurysms,” *European Radiology* 31, no. 5 (2021): 2716–2725.
 55. C. G. Ludwig, A. Lauric, J. A. Malek, R. Mulligan, and A. M. Malek, “Performance of Radiomics Derived Morphological Features for Prediction of Aneurysm Rupture Status,” *Journal of NeuroInterventional Surgery* 13, no. 8 (2021): 755–761.
 56. W. Zhu, W. Li, Z. Tian, et al., “Stability Assessment of Intracranial Aneurysms Using Machine Learning Based on Clinical and Morphological Features,” *Translational Stroke Research* 11, no. 6 (2020): 1287–1295.
 57. H. Lu, G. Xue, S. Li, et al., “An Accurate Prognostic Prediction for Aneurysmal Subarachnoid Hemorrhage Dedicated to Patients After Endovascular Treatment,” *Therapeutic Advances in Neurological Disorders* 15 (2022), <https://doi.org/10.1177/17562864221099473>.
 58. K. Wu, D. Gu, P. Qi, et al., “Evaluation of an Automated Intracranial Aneurysm Detection and Rupture Analysis Approach Using Cascade Detection and Classification Networks,” *Computerized Medical Imaging and Graphics* 102 (2022): 102126.
 59. Y. Li, L. Huan, W. Lu, et al., “Integrate Prediction of Machine Learning for Single ACoA Rupture Risk: A Multicenter Retrospective Analysis,” *Frontiers in Neurology* 14 (2023): 1126640.

60. N. Paliwal, P. Jaiswal, V. M. Tutino, et al., "Outcome Prediction of Intracranial Aneurysm Treatment by Flow Diverters Using Machine Learning," *Neurosurgical Focus* 45, no. 5 (2018): E7.
61. J. H. Ahn, H. C. Kim, J. K. Rhim, et al., "Multi-View Convolutional Neural Networks in Rupture Risk Assessment of Small, Unruptured Intracranial Aneurysms," *Journal of Personalized Medicine* 11, no. 4 (2021): 239.
62. A. Jadhav, S. Kashyap, H. Bulu, et al., "Towards Automatic Prediction of Outcome in Treatment of Cerebral Aneurysms," *AMIA Annual Symposium Proceedings* 2022 (2022): 570–579.
63. D. Kong, J. Li, Y. Lv, et al., "Radiomics Nomogram Model Based on TOF-MRA Images: A New Effective Method for Predicting Microaneurysms," *International Journal of General Medicine* 16 (2023): 1091–1100.
64. H. Jin, J. Geng, Y. Yin, et al., "Fully Automated Intracranial Aneurysm Detection and Segmentation From Digital Subtraction Angiography Series Using an End-to-End Spatiotemporal Deep Neural Network," *Journal of NeuroInterventional Surgery* 12, no. 10 (2020): 1023–1027.
65. N. Lv, C. Karmonik, Z. Shi, et al., "A Pilot Study Using a Machine-Learning Approach of Morphological and Hemodynamic Parameters for Predicting Aneurysms Enhancement," *International Journal of Computer Assisted Radiology and Surgery* 15, no. 8 (2020): 1313–1321.
66. G. Chen, M. Lu, Z. Shi, et al., "Development and Validation of Machine Learning Prediction Model Based on Computed Tomography Angiography-Derived Hemodynamics for Rupture Status of Intracranial Aneurysms: A Chinese Multicenter Study," *European Radiology* 30, no. 9 (2020): 5170–5182.
67. J. Feng, R. Zeng, Y. Geng, et al., "Automatic Differentiation of Ruptured and Unruptured Intracranial Aneurysms on Computed Tomography Angiography Based on Deep Learning and Radiomics," *Insights Imaging* 14, no. 1 (2023): 76.
68. R. Li, P. Zhou, X. Chen, M. Mossa-Basha, C. Zhu, and Y. Wang, "Construction and Evaluation of Multiple Radiomics Models for Identifying the Instability of Intracranial Aneurysms Based on CTA," *Frontiers in Neurology* 13 (2022): 876238.
69. Z. Tian, W. Li, X. Feng, K. Sun, and C. Duan, "Prediction and Analysis of Periprocedural Complications Associated With Endovascular Treatment for Unruptured Intracranial Aneurysms Using Machine Learning," *Frontiers in Neurology* 13 (2022): 1027557.
70. S. F. Salimi Ashkezari, F. Mut, M. Slawski, et al., "Prediction of Bleb Formation in Intracranial Aneurysms Using Machine Learning Models Based on Aneurysm Hemodynamics, Geometry, Location, and Patient Population," *Journal of NeuroInterventional Surgery* 14, no. 10 (2022): 1002–1007.
71. J. Liu, Y. Chen, D. Zhu, et al., "A Nomogram to Predict Rupture Risk of Middle Cerebral Artery Aneurysm," *Neurological Sciences* 42, no. 12 (2021): 5289–5296.
72. L. Zeng, X. Y. Zhao, L. Wen, et al., "Compare Deep Learning Model and Conventional Logistic Regression Model for the Identification of Unstable Saccular Intracranial Aneurysms in Computed Tomography Angiography," *Quantitative Imaging in Medicine and Surgery* 14, no. 4 (2024): 2993–3005.
73. H. Cao, H. Zeng, L. Lv, et al., "Assessment of Intracranial Aneurysm Rupture Risk Using a Point Cloud-Based Deep Learning Model," *Frontiers in Physiology* 15 (2024): 1293380.
74. M. Irfan, K. M. Malik, J. Ahmad, and G. Malik, "StrokeNet: An Automated Approach for Segmentation and Rupture Risk Prediction of Intracranial Aneurysm," *Computerized Medical Imaging and Graphics* 108 (2023): 102271.
75. M. M. Shiraz Bhurwani, M. Waqas, A. R. Podgorsak, et al., "Feasibility Study for Use of Angiographic Parametric Imaging and Deep Neural Networks for Intracranial Aneurysm Occlusion Prediction," *Journal of NeuroInterventional Surgery* 12, no. 7 (2020): 714–719.
76. S. S. Veeturi, A. Saleem, D. Ojeda, et al., "Radiomics-Based Predictive Nomogram for Assessing the Risk of Intracranial Aneurysms," *Research Square* 16 (2024): 79–87, <https://doi.org/10.1007/s12975-024-01268-3>.
77. S. Hadad, F. Mut, M. Slawski, A. M. Robertson, and J. R. Cebal, "Evaluation of Predictive Models of Aneurysm Focal Growth and Bleb Development Using Machine Learning Techniques," *Journal of NeuroInterventional Surgery* 16, no. 4 (2024): 392–397.
78. H. Jin, J. Lv, C. Li, et al., "Morphological Features Predicting In-Stent Stenosis After Pipeline Implantation for Unruptured Intracranial Aneurysm," *Frontiers in Neurology* 14 (2023): 1121134.
79. X. Tong, X. Feng, F. Peng, et al., "Rupture Discrimination of Multiple Small (< 7 mm) Intracranial Aneurysms Based on Machine Learning-Based Cluster Analysis," *BMC Neurology* 23, no. 1 (2023): 45.
80. Y. Ye, J. Chen, X. Qiu, et al., "Prediction of Small Intracranial Aneurysm Rupture Status Based on Combined Clinical-Radiomics Model," *Heliyon* 10, no. 9 (2024): e30214.
81. C. Ma, S. Liang, F. Liang, et al., "Predicting Postinterventional Rupture of Intracranial Aneurysms Using Arteriography-Derived Radiomic Features After Pipeline Embolization," *Frontiers in Neurology* 15 (2024): 1327127.
82. Z. Zador, W. Huang, M. Sperrin, and M. T. Lawton, "Multivariable and Bayesian Network Analysis of Outcome Predictors in Acute Aneurysmal Subarachnoid Hemorrhage: Review of a Pure Surgical Series in the Post-International Subarachnoid Aneurysm Trial Era," *Operative Neurosurgery* 14, no. 6 (2018): 603–610.
83. K. Sunderland, M. Wang, A. S. Pandey, et al., "Quantitative Analysis of Flow Vortices: Differentiation of Unruptured and Ruptured Medium-Sized Middle Cerebral Artery Aneurysms," *Acta Neurochirurgica* 163, no. 8 (2021): 2339–2349.
84. X. Cao, W. Xia, Y. Tang, et al., "Radiomic Model for Distinguishing Dissecting Aneurysms From Complicated Saccular Aneurysms on High-Resolution Magnetic Resonance Imaging," *Journal of Stroke and Cerebrovascular Diseases* 29, no. 12 (2020): 105268.
85. B. Hammoud, J. El Zini, M. Awad, A. Sweid, S. Tjoumakaris, and P. Jabbour, "Predicting Incomplete Occlusion of Intracranial Aneurysms Treated With Flow Diverters Using Machine Learning Models," *Journal of Neurosurgery* 140, no. 6 (2024): 1716–1725.
86. A. Guédon, C. Thépenier, E. Shotar, et al., "Predictive Score for Complete Occlusion of Intracranial Aneurysms Treated by Flow-Diverter Stents Using Machine Learning," *Journal of NeuroInterventional Surgery* 13, no. 4 (2021): 341–346.
87. Z. H. Bo, H. Qiao, C. Tian, et al., "Toward Human Intervention-Free Clinical Diagnosis of Intracranial Aneurysm via Deep Neural Network," *Patterns* 2, no. 2 (2021): 100197.
88. A. G. Wisniewski, M. M. Shiraz Bhurwani, K. N. Sommer, et al., "Quantitative Angiography Prognosis of Intracranial Aneurysm Treatment Failure Using Parametric Imaging and Distal Vessel Analysis," *Proceedings of SPIE: The International Society for Optical Engineering* 12036 (2022): 120360D.
89. W. Li, X. Wu, J. Wang, et al., "A Novel Clinical-Radscore Nomogram for Predicting Ruptured Intracranial Aneurysm," *Heliyon* 9, no. 10 (2023): e20718.
90. X. Luo, J. Wang, X. Liang, et al., "Prediction of Cerebral Aneurysm Rupture Using a Point Cloud Neural Network," *Journal of NeuroInterventional Surgery* 15, no. 4 (2023): 380–386.
91. G. Zhu, X. Luo, T. Yang, et al., "Deep Learning-Based Recognition and Segmentation of Intracranial Aneurysms Under Small Sample Size," *Frontiers in Physiology* 13 (2022): 1084202.
92. M. Turhon, M. Li, H. Kang, et al., "Development and Validation of a Deep Learning Model for Prediction of Intracranial Aneurysm Rupture Risk Based on Multi-Omics Factor," *European Radiology* 33, no. 10 (2023): 6759–6770.

93. S. S. Veeturi, T. R. Patel, A. A. Baig, et al., "Hemodynamic Analysis Shows High Wall Shear Stress Is Associated With Intraoperatively Observed Thin Wall Regions of Intracranial Aneurysms," *Journal of Cardiovascular Development and Disease* 9, no. 12 (2022): 424.
94. M. Ishibashi, K. Egashira, Q. Zhao, et al., "Bone Marrow-Derived Monocyte Chemoattractant Protein-1 Receptor CCR2 Is Critical in Angiotensin II-Induced Acceleration of Atherosclerosis and Aneurysm Formation in Hypercholesterolemic Mice," *Arteriosclerosis, Thrombosis, and Vascular Biology* 24, no. 11 (2004): e174–e178.
95. C. Chen, F. Tang, M. Zhu, et al., "Role of Inflammatory Mediators in Intracranial Aneurysms: A Review," *Clinical Neurology and Neurosurgery* 242 (2024): 108329.
96. T. W. Anderson and D. A. Darling, "Asymptotic Theory of Certain "Goodness of Fit" Criteria Based on Stochastic Processes," *The Annals of Mathematical Statistics* 23, no. 2 (1952): 193–212.
97. J. Liu, Y. Chen, L. Lan, et al., "Prediction of Rupture Risk in Anterior Communicating Artery Aneurysms With a Feed-Forward Artificial Neural Network," *European Radiology* 28, no. 8 (2018): 3268–3275.